

# East-west extension and Miocene environmental change in the southern Tibetan plateau: Thakkhola graben, central Nepal

Carmala N. Garzione<sup>†</sup>

*Department of Earth and Environmental Sciences, University of Rochester, Rochester, New York 14627, USA*

Peter G. DeCelles

Damian G. Hodkinson

Tank P. Ojha

*Department of Geosciences, University of Arizona, Tucson, Arizona 85721, USA*

Bishal N. Upreti

*Department of Geology, Tribhuvan University, Tri-Chandra Campus, Ghantaghar, Kathmandu, Nepal*

## ABSTRACT

East-west extensional basins are distributed across the southern half of the Tibetan plateau at an elevation of ~4 km. These basins have generated much interest because of their potential implications for the regional tectonics and force distribution in the plateau. This study documents the sedimentology of the Miocene–Pliocene Thakkhola graben fill in order to reconstruct basin evolution and paleoenvironment. Analysis of depositional systems, paleo-drainage patterns, and conglomerate clast provenance of the >1-km-thick graben fill sets limits on the timing of activity of the basin-bounding faults and the development of southward axial drainage in the basin. During the deposition of the oldest basin fill (Tetang Formation, ca. 11–9.6 Ma), probably in a restricted basin, minor motion occurred on the basin-bounding fault systems. An angular unconformity separates the Tetang and overlying Thakkhola Formations, where this contact can be observed in the southern part of the basin. Southward axial drainage was established by ca. 7 Ma with the onset of deposition of the Thakkhola Formation. Several episodes of damming of this drainage system are recorded by widespread lacustrine deposits in the southern part of the basin. Facies distribution and the progressive rotation of strata in the Thakkhola Formation indicate that the Dangardzong fault on the western edge of the basin was active at this time, and drain-

age ponding may have been related to displacement on normal faults associated with the South Tibetan detachment system to the south of Thakkhola graben.

Contrasts between deposits of the Tetang and Thakkhola Formations provide evidence for environmental change in the basin. In the Tetang Formation, the abundance of lacustrine facies, the pollen record, and the absence of paleosol carbonate suggest that conditions were more humid than during subsequent deposition of the Thakkhola Formation. Environmental change in the Thakkhola graben coincided with environmental change observed in the Siwalik foreland basin sequence, Arabian Sea, and Bay of Bengal at ca. 8–7 Ma. Although this climate change event has been previously attributed to intensification of the Asian monsoon in response to uplift of the Tibetan plateau, paleoaltimetry data indicate that this region had already attained a high elevation by ca. 11 Ma. Thus, the Thakkhola graben stratigraphic record suggests that uplift of the southern Tibetan plateau and the onset of the Asian monsoon as inferred from paleoclimatic indicators were not directly related in a simple way.

**Keywords:** extension, Nepal, Thakkhola graben, Tibetan plateau.

## INTRODUCTION

Normal faults and grabens indicating generally east-west extension are distributed throughout the southern half of the Tibetan

plateau (Fig. 1). Since their discovery (Molnar and Tapponnier, 1978; Ni and York, 1978), geologists and geophysicists have speculated on the origins of these seemingly enigmatic features in a regionally contractional tectonic setting between the colliding Indian and Eurasian plates. The list of possible causes includes (1) upper-crustal gravitational failure in response to the attainment of high elevation on the plateau (Molnar and Tapponnier, 1978; Molnar and Lyon-Caen, 1988), (2) extension in response to regional, conjugate strike-slip faulting associated with eastward extrusion of Tibet (Armijo et al., 1986), (3) isostatic response to erosion of the mantle lithosphere below Tibet (England and Houseman, 1989), (4) lower-crustal flow (Royden et al., 1997), (5) oblique convergence between India and Asia (McCaffrey and Nabelek, 1998), (6) arc-parallel extension (Seeber and Pêcher, 1998), and (7) middle Tertiary mantle upwelling in eastern Asia that induced thermal weakening of the lithosphere (Yin, 2000).

Indirect evidence of the timing of initiation of east-west extension comes from the dating of mineral and whole-rock samples from veins and north-trending dikes thought to be associated with east-west extension. These dates suggest older ages of ca. 14 Ma for a vein in the Tethyan Himalaya (Coleman and Hodges, 1995),  $18.3 \pm 2.7$  Ma for ultrapotassic dikes in the Lhasa terrane (Williams et al., 2001), and ca. 13.5 Ma for fault zone mineralization in the Shuang Hu graben in the Qiangtang terrane in central Tibet (Blisniuk et al., 2001). A younger estimate of ca. 4 Ma for the initiation of extension in the Shuang Hu graben was ob-

<sup>†</sup>E-mail: garzione@earth.rochester.edu.

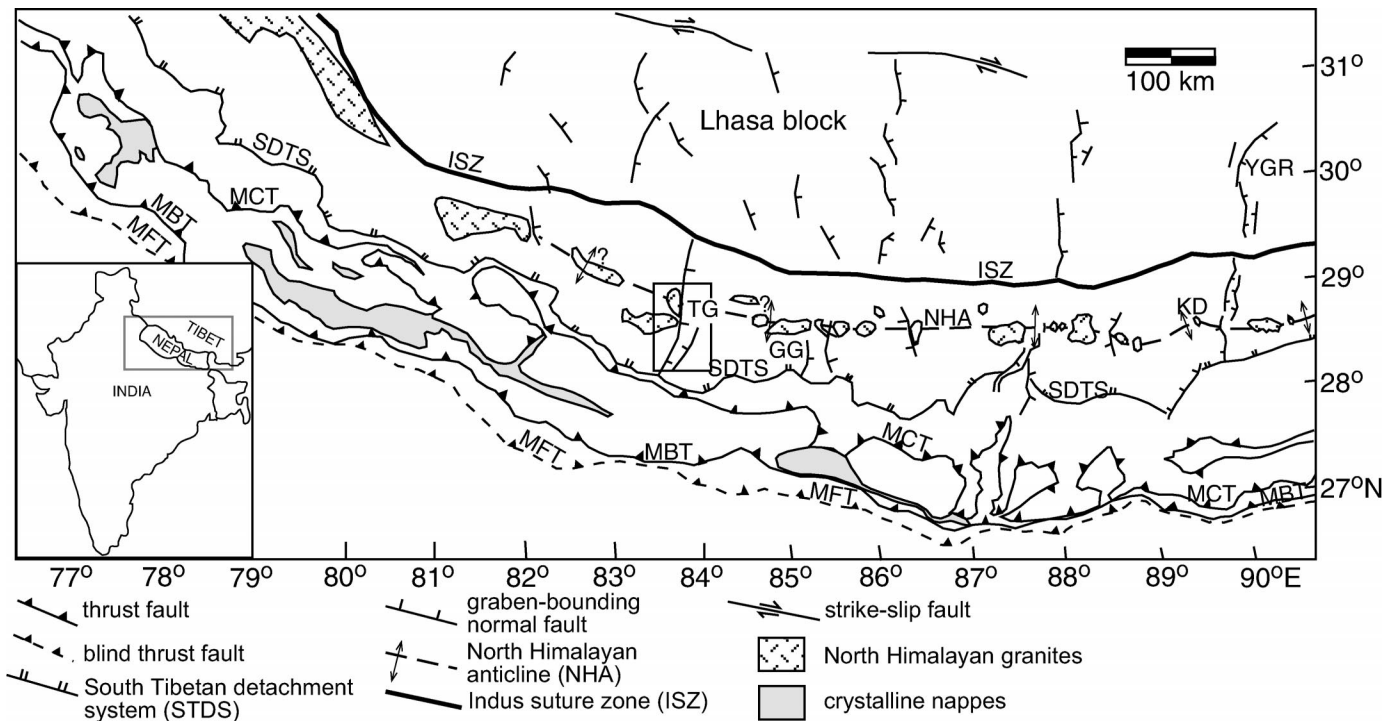


**Figure 1.** General tectonic map of southern Tibetan plateau and Nepal Himalaya, modified from Hodges (2000) and Hauck et al. (1998). Features: Main Central thrust (MCT), Main Boundary thrust (MBT), Main Frontal thrust (MFT), Thakkhola graben (TG), Gyirong graben (GG), Yadong-Gulu rift (YGR), Kangmar dome (KD). Box shows location of study area detailed in Figure 2. Inset is a smaller-scale political map of the region; the gray rectangle shows the location of the tectonic map.

tained by using Holocene slip rates to determine the time required to produce the total displacement on the major graben-bounding fault (Yin et al., 1999). More direct chronological constraints on the beginning of east-west extension come from a thermochronological study of the shear zone that bounds the western edge of the Yangbajian graben in the southeastern part of the plateau (Fig. 1), where a phase of rapid exhumation, inferred to indicate extension, took place between ca. 8 Ma and 3 Ma (Pan and Kidd, 1992; Harrison et al., 1995). The link between high elevation and late Miocene east-west extension (beginning ca. 8 Ma) is supported by a regionally documented paleoclimate event that has been inferred to correlate with the intensification of the south Asian monsoon (Quade et al., 1989; Hoorn et al., 2000) and changes in oceanic upwelling conditions (Kroon et al., 1991; Prell et al., 1992). However, the relationship between high-elevation-driven climate change and regional east-west extension has not been seriously examined in any of the graben fills.

The argument linking extension to late Miocene climate change led Garzione et al. (2000a, 2000b) to document the paleoelevation history of the Thakkhola graben in north-central Nepal (Fig. 1) with oxygen isotope

data from lacustrine and paleosol carbonates. Those data suggest that the basin floor was already at an elevation of ~4 km by ca. 11 Ma. In this paper we document the sedimentology and provenance of the Thakkhola basin fill in order to reconstruct the paleogeography of the basin fill and shed new light on the nature of east-west extension in the southern part of the plateau.

### GEOLOGIC SETTING

The Thakkhola graben, in north-central Nepal, formed in Paleozoic to Cretaceous rocks of the Tethyan Series between the South Tibetan detachment system to the south and the Indus suture zone to the north (Fig. 1). The South Tibetan detachment system is a low-angle, north-dipping, normal-fault system located in the highest part of the Himalaya (Burg and Chen, 1984; Burchfiel et al., 1992; Godin et al., 1999). On the basis of the uniformly high elevation north of the South Tibetan detachment system (Fielding et al., 1994), this area is considered to be part of the Tibetan plateau. However, the Indus suture zone marks the boundary between the Indian and Eurasia plates, so the area south of the suture is also

part of the Himalayan fold-thrust belt (Gansser, 1964; Searle, 1986).

The kinematic history of the Himalayan fold-thrust belt followed a generally southward progression of emplacement of the major thrust systems (Schelling, 1992; Srivastava and Mitra, 1994; DeCelles et al., 1998, 2001) (Fig. 1). Tibetan thrusts were active mainly during Eocene and Oligocene time (Searle, 1986; Ratschbacher et al., 1994) and produced regional Barrovian metamorphism of the underlying Greater Himalayan rocks (Hodges and Silverburg, 1988; Vannay and Hodges, 1996; Coleman, 1998; Guillot, 1999; Catlos et al., 2001). Thermochronologic data from the Greater Himalayan rocks suggest rapid cooling during early Miocene time (since ca. 22.5 Ma), presumably during emplacement of the Main Central thrust system (Hubbard and Harrison, 1989; Hodges et al., 1996; Coleman, 1998). At about the same time, the South Tibetan detachment system became active, dropping Tethyan Series rocks downward to the north against Greater Himalayan rocks in the footwall (Hodges et al., 1996; Coleman, 1998; Godin et al., 1999; Murphy and Harrison, 1999). Since middle Miocene time the front of the fold-thrust belt has propagated southward into the Lesser Himalayan and Subhi-

malayan zones (Mugnier et al., 1993; DeCelles et al., 2001). Several major thrust systems, including the Ramgarh thrust, have built a large duplex in Lesser Himalayan rocks to the south of the Main Central thrust. Situated on top of the Lesser Himalaya are isolated, synformal thrust sheets commonly called the crystalline nappes. These are interpreted to be the southern continuations of the Greater Himalayan zone (Gansser, 1964; Stöcklin, 1980; Valdiya, 1980; Johnson et al., 2001), which have been folded into synformal structures during growth of the Lesser Himalayan duplex (Schelling, 1992; Srivastava and Mitra, 1994; DeCelles et al., 2001). The Main Boundary thrust places Lesser Himalayan quartzite and phyllite against the Neogene Siwalik Group of the Subhimalayan zone (Dhital and Kizaki, 1987; Schelling, 1992; Srivastava and Mitra, 1994). Provenance data from these foreland basin deposits indicate large-scale unroofing of the crystalline nappes beginning at ca. 11 Ma, which suggests that the Lesser Himalayan duplex that folded the crystalline nappes began growing at that time (DeCelles et al., 1998).

The Thakkhola graben is bounded by Paleozoic Tethyan Series rocks in its western footwall and Mesozoic Tethyan Series rocks in its eastern footwall (Fig. 2). Different levels of exposure between the eastern and western footwalls reflect greater displacement along the western basin-bounding fault (Fort et al., 1982; Colchen et al., 1986; Colchen, 1999). The Mustang and Mugu granites are exposed along the western edge of the basin. These are part of the North Himalayan granite belt, exposed midway between the South Tibetan detachment system and the Indus suture zone (Fig. 1) (Le Fort, 1986; Le Fort and France-Lanord, 1995). The North Himalayan granites range in age from ca. 10 Ma to ca. 17 Ma, and the Mugu pluton has been dated by Th-Pb monazite at  $17.6 \pm 0.3$  Ma (Harrison et al., 1997).

Two formations have been mapped in Thakkhola graben. The older Tetang Formation is up to 240 m thick and crops out in the southeastern part of the basin, where the entire basin fill has been incised (Fig. 2). The Tetang Formation rests unconformably on previously folded and faulted Tethyan Series rocks. The best estimate for the age range of the Tetang Formation is between ca. 11 and 9.6 Ma, based on magnetostratigraphy (Garzzone et al., 2000a). An older age (ca. 14 Ma) for extension in the Thakkhola graben was inferred from an  $^{40}\text{Ar}/^{39}\text{Ar}$  mica date from a vein associated with a north-striking normal fault

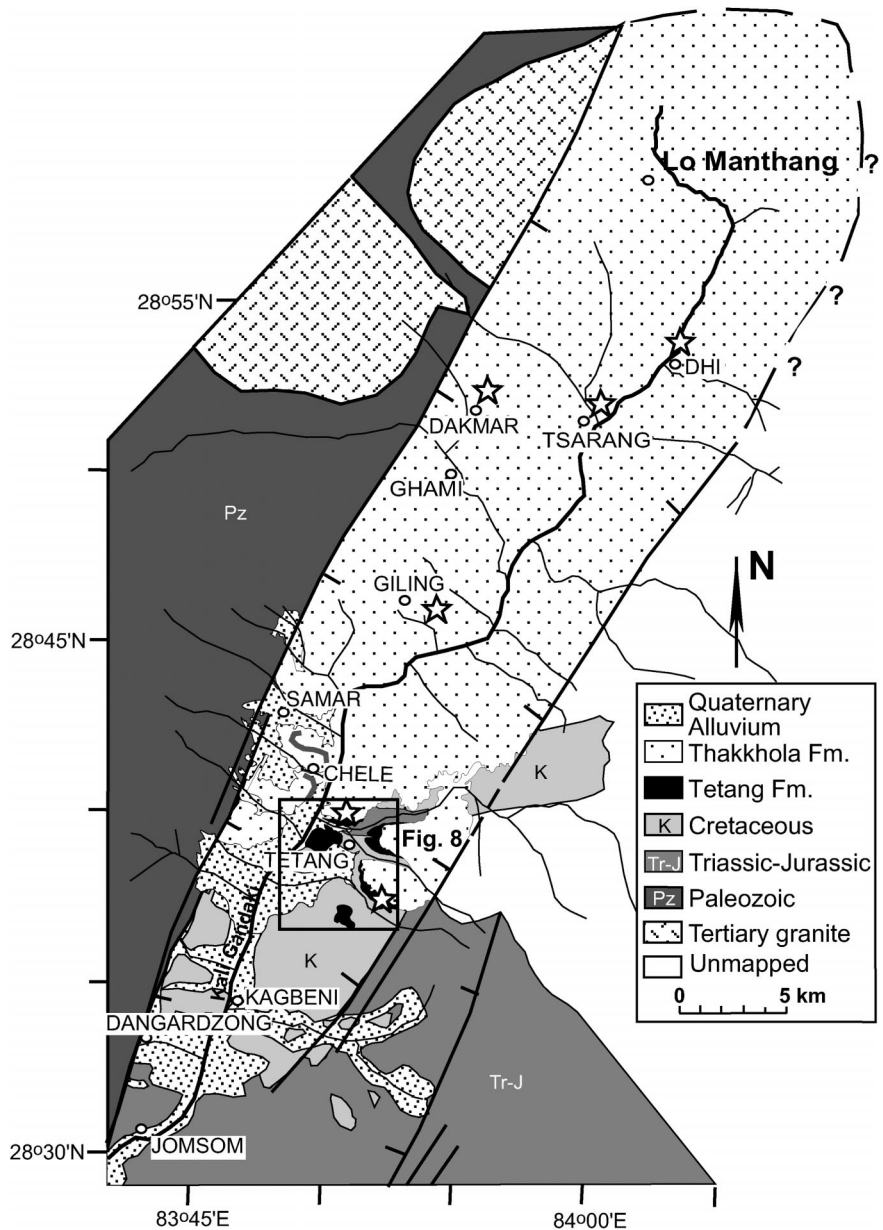


**Figure 2.** Geologic map of Thakkhola graben modified from Fort et al. (1982) and Colchen et al. (1986), showing locations of measured sections (stars and thick gray lines, near Chele).

along the Marsyangdi valley in central Nepal (Coleman and Hodges, 1995).

An angular unconformity marks the contact between the Tetang Formation and the overlying Thakkhola Formation (Fort et al., 1981). The Thakkhola Formation crops out throughout the basin and is up to ~1000 m thick. Stable carbon isotopic data from paleosol carbonate nodules of the Thakkhola Formation indicate the presence of  $C_4$  grasses in the basin throughout deposition of the Thakkhola Formation (Garzzone et al., 2000a). Global expansion of  $C_4$  grasses took place between 8

and 6 Ma (Cerling et al., 1997) and did not appear in the south Asian soil carbonate record until ca. 7 Ma (Quade et al., 1989, 1995), which suggests an age of younger than 7 Ma for deposition of the Thakkhola Formation. Oxygen isotopes of lacustrine and paleosol carbonate rocks in the Thakkhola graben indicate elevations consistent with modern elevations since deposition began in the basin (Garzzone et al., 2000a, 2000b).

Today, the Kali Gandaki river locally drains the southern Tibetan plateau, flowing southward along the axis of the Thakkhola graben,

through the fold-thrust belt to the Himalayan foreland. Terrace deposits in the Kali Gandaki valley document multiple phases of Quaternary damming and incision (e.g., Fort et al., 1982; Iwata, 1984; Hurtado et al., 2001).

### SEDIMENTOLOGY OF THE TETANG AND THAKKHOLA FORMATIONS

Environments of deposition are interpreted on the basis of six, bed-by-bed measured sections in the Thakkhola graben (Figs. 2, 3, and 4). The ~240-m-thick Tetang Formation crops out in the southeastern part of the basin and fines upward from alluvial-fan and braided fluvial conglomerates into lacustrine mudstone and carbonate (Fig. 3). The Thakkhola Formation, which is distributed throughout the basin, is at least ~800 m thick and generally fines upward from alluvial-fan and braided fluvial conglomerate to lacustrine mudstone and carbonate and braided fluvial conglomerate (Fig. 4). Each measured section is separated by >5 km distance. Minor faults, synthetic to the eastern and western basin-bounding faults, have displacements of several tens to hundreds of meters and offset sections of the Tetang and Thakkhola Formations, precluding precise correlations between sections. Within these sections, we counted >2600 clasts to determine provenance and measured >710 paleocurrent indicators. Paleocurrent directions were determined from imbricated gravels. Ten or more clast orientations were measured in individual beds. Conglomerate provenance was determined by counting 100 or more clasts from each site. Clasts were recorded by rock type and description and classified as Paleozoic, Mesozoic, and Tertiary granite, on the basis of our observations of these units along the margins of the basin. Paleocurrent and provenance data are shown on the stratigraphic columns (Figs. 3 and 4). Excellent lateral continuity of exposures allowed for two-dimensional observations of depositional architecture and facies associations over hundreds of meters to several kilometers. Stratigraphic sections indicate three genetic lithofacies associations: alluvial fan, braided stream, and lacustrine.

#### Alluvial-fan Lithofacies Association

##### Description

Dominantly conglomeratic sections of the alluvial-fan lithofacies association, up to 400 m thick, are exposed along the western and southeastern edges of the basin. The alluvial-fan lithofacies association consists of five lithofacies: A1–A5.

Lithofacies A1 is moderately sorted, clast-supported, granule-boulder conglomerate (Fig. 5A). Clasts are subangular to subrounded. Conglomerate beds are 0.3–2 m thick, have erosive bases, and can be traced laterally for tens to hundreds of meters. Deposits are generally massive but also have local clast imbrication and crude horizontal stratification. No overall vertical trends in grain size are evident in these conglomerate bodies.

Lithofacies A2 consists of poorly sorted, matrix- or clast-supported, cobble-boulder conglomerate (Fig. 5A). Clasts are angular and are supported by a matrix of silt- to sand-sized grains. Individual beds are 0.5–4 m thick, extend laterally for tens of meters, and have nonerosive bases. Beds of lithofacies A2 lack stratification but locally exhibit inverse grading.

Lithofacies A3 comprises imbricated to massive, moderately well sorted, pebble-cobble conglomerates. These conglomerates are clast supported and consist of rounded clasts in a sand-sized matrix. The deposits occur in 1–20-m-thick, multistory lenticular bodies with erosive bases that continue laterally for up to 100 m or more. Lenticular beds are 0.2–3 m thick and extend laterally for tens of meters and are sometimes deeply inset within adjacent deposits.

Lithofacies A4 consists of wedge-shaped bodies of structureless or horizontally laminated, fine-grained to very coarse grained sandstone (Fig. 5B). Scour and fill structures are common. These deposits form 0.1–1-m-thick lenticular beds that continue laterally for up to 10 m and are associated with imbricated, pebble-cobble conglomerates of facies A3.

Lithofacies A5 is a minor component of the alluvial-fan facies that is associated with all of the above lithofacies and consists of massive, completely unstratified, red sandy mudstone with angular, matrix-supported clasts up to pebble size. These beds can be traced laterally for hundreds of meters and are generally <1 m thick. They are often mottled and rarely contain diffuse nodular carbonate (<1 cm diameter) horizons.

##### Interpretation

We interpret lithofacies A1 as unconfined sheetflood deposits. Horizontal stratification and imbrication suggest that clasts were transported in traction flows. Many authors have interpreted similar alluvial-fan facies as the deposits of hyperconcentrated flood flows (e.g., Nemeč and Steel, 1984; Horton and Schmitt, 1996).

Lithofacies A2 is interpreted as debris flows. Clast-supported, inversely graded beds

indicate that dispersive forces were significant, perhaps during transport as density-modified grain flows and/or clast-rich debris flows (e.g., Nemeč and Steel, 1984). Another possibility is that these inversely graded beds were deposited as gravelly traction carpets, a type of shear modified grain flow (Todd, 1989; Sohn, 1997).

Lithofacies A3 has channel-fill geometries that suggest it is fluvial channel fill deposited in fan channel networks or incised fanhead trenches (e.g., DeCelles et al., 1991). In association with channel-fill deposits, lithofacies A4 is interpreted as sand wedges that accumulated on bar flanks, deposited during waning flow.

We interpret lithofacies A5 as paleosols that formed on temporarily abandoned parts of the alluvial fan.

#### Braided River Lithofacies Association

##### Description

The braided stream lithofacies association consists of three lithofacies. Sections of interbedded clast-supported conglomerate (B1), sandstone (B2), and mudstone (B3), between 10 and 400 m thick, are exposed throughout the Thakkhola basin. The primary braided stream lithofacies (B1) consists of moderately sorted, clast-supported, pebble-cobble conglomerate. Clasts are well rounded and are usually imbricated or horizontally stratified (Fig. 5C). Conglomerate deposits form 0.1–2-m-thick lenticular beds that extend laterally for 3 to >50 m. These beds stack to form lenticular bodies that extend laterally for tens of meters to >1 km. Thicker, more laterally extensive pebbly beds display trough cross-stratification. Beds have sharp or scoured bases and commonly fine upward. Coarser cobble conglomerates are concentrated in the axis of the Thakkhola basin.

Lithofacies B2 is moderately to poorly sorted, massive or weakly horizontally laminated sandstone/mudstone and commonly displays scour and fill structures or cross-stratification. Grain size varies from silt to very coarse sand, and floating pebbles are common. These sandstone beds are <0.1–0.5 m thick, continue laterally for tens of meters, and are interbedded with conglomerate deposits of lithofacies B1. Sandstone grain size usually fines upward, and sandstone often caps a fining-upward conglomerate. Conglomerate and sandstone form multistory lenticular bodies between 1 and 12 m thick.

Lithofacies B3 separates bodies of lithofacies B1 and B2, consisting of laminated or massive mudstone. Laminated mudstone is



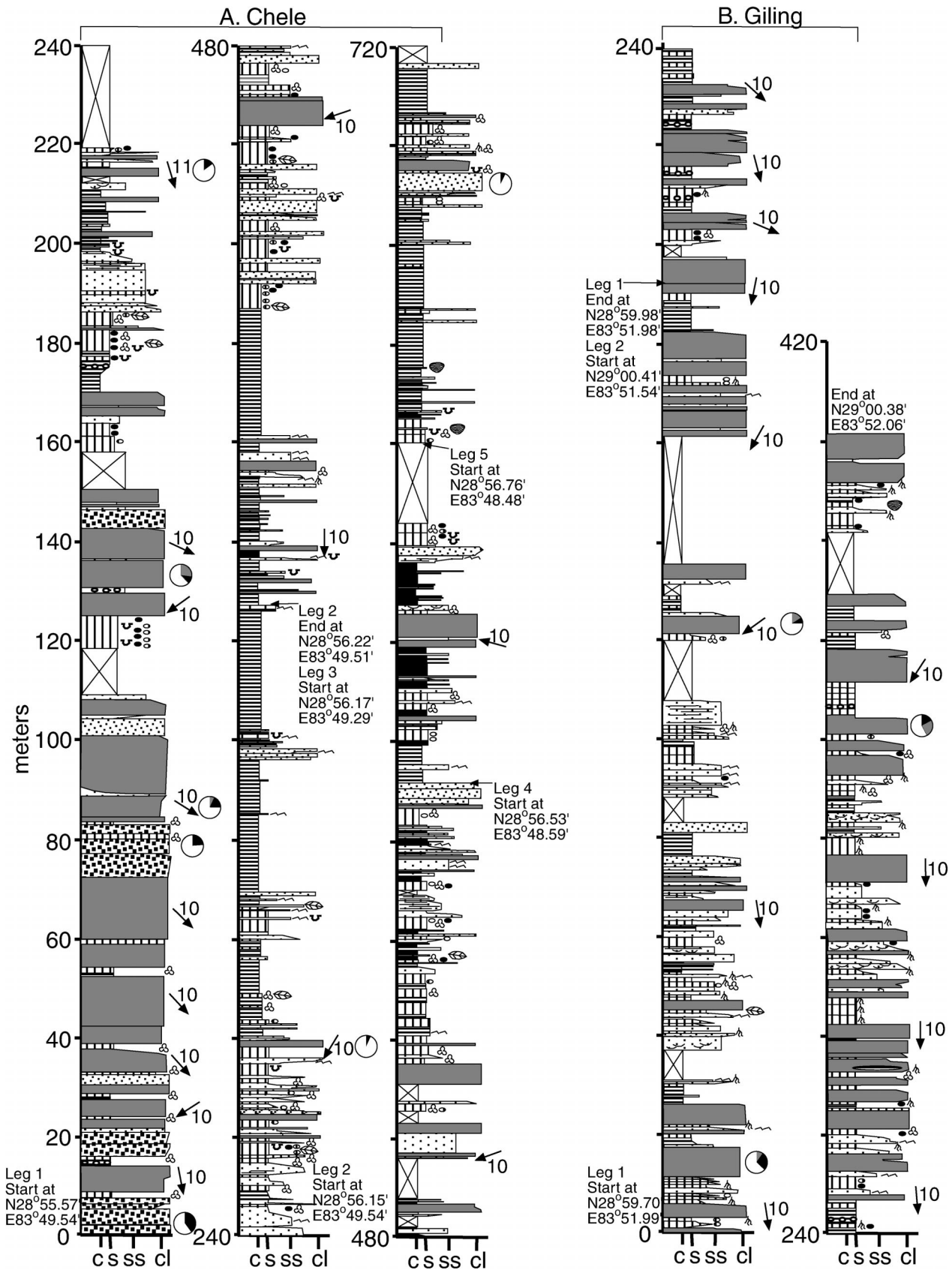


Figure 4. Logs of measured stratigraphic sections of the Thakkhola Formation near (A) Chele village, (B) Giling village, (C) Dakmar village, and (D) Dhi village. (E) Paleoflow directions based on imbricated clasts measured in axial braided river facies along Tsarang Khola (see Fig. 2 for location).

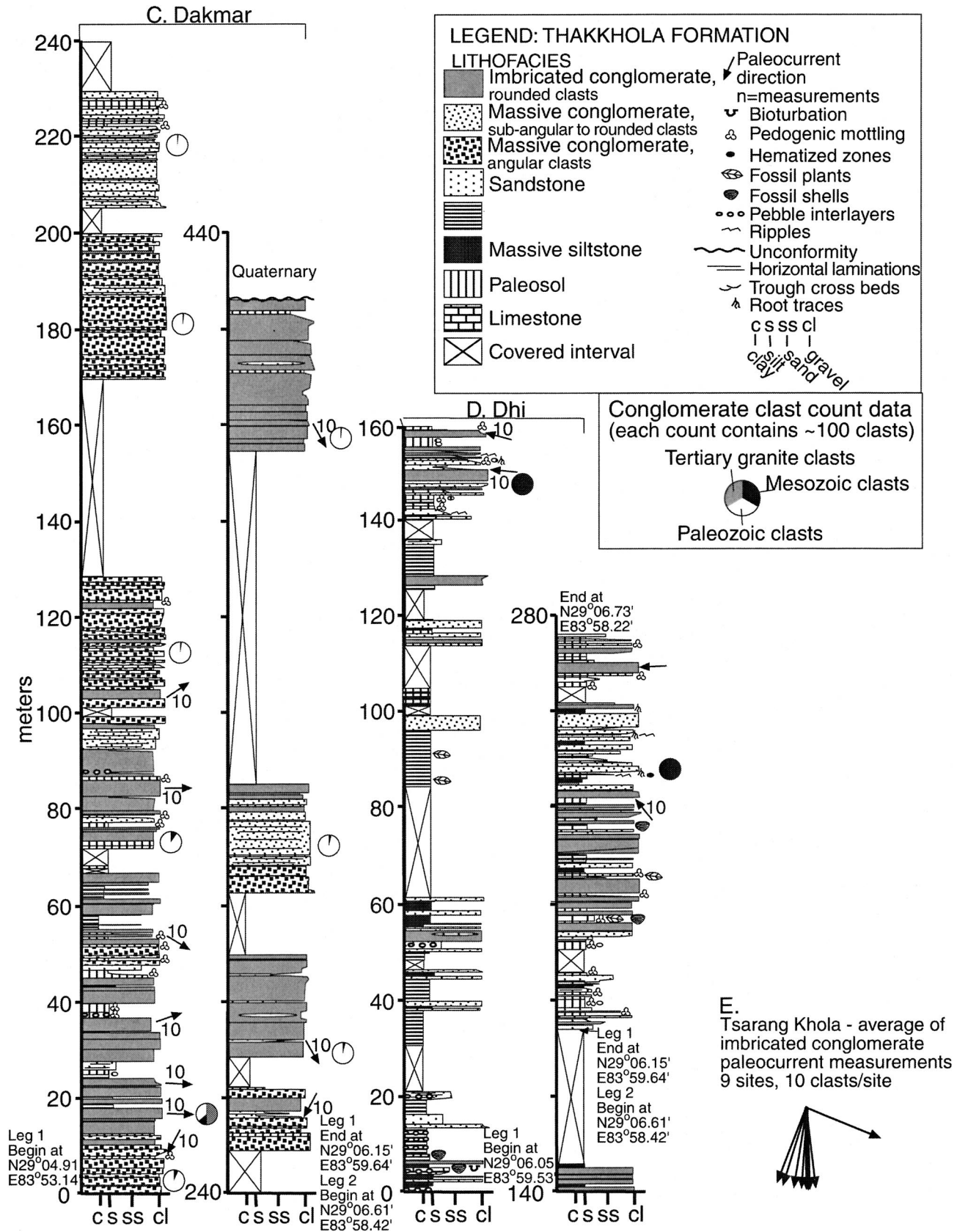
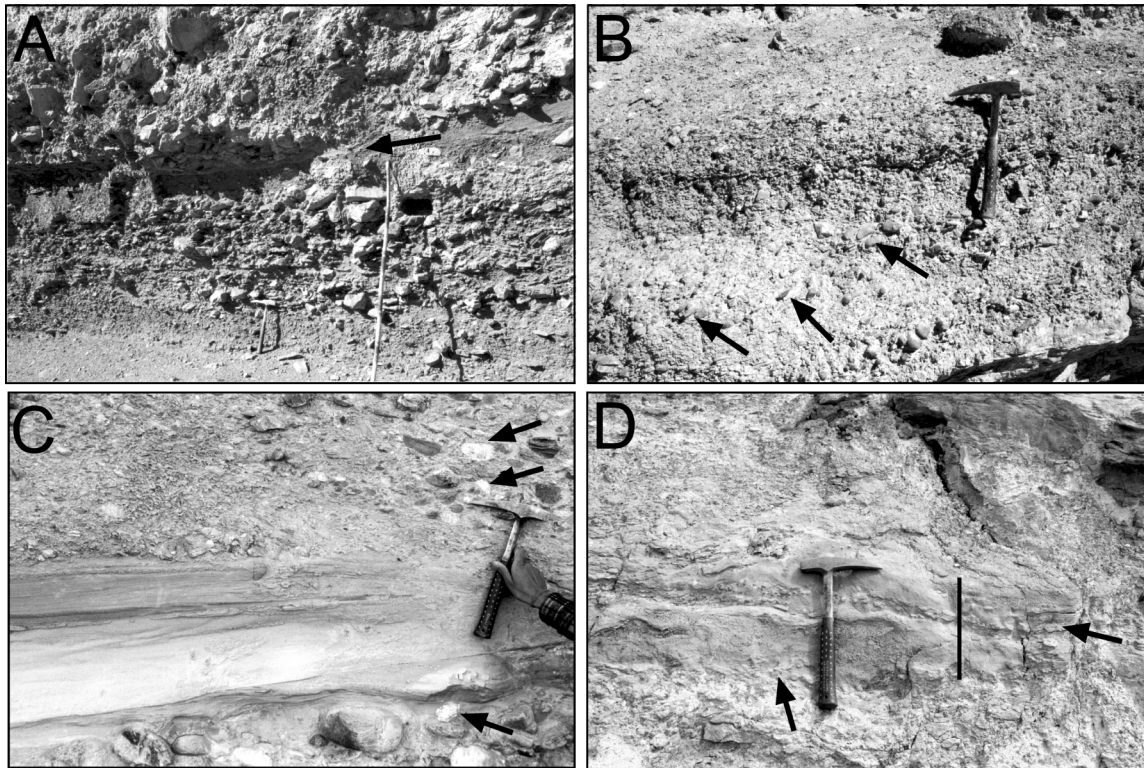


Figure 4. (Continued.)



**Figure 5.** Examples of lithofacies; 35-cm-long hammer for scale. (A) Sheetflood and debris-flow deposits of facies A1 and A2 of alluvial-fan facies association. Thakkhola Formation, near Chele village (Fig. 4A). Arrow points to contact between water-transported deposits below and debris-flow deposits above. Lower bed has dark red paleosol development in upper 20 cm of bed. (B) Imbricated pebbly fluvial conglomerate of facies B1 of braided fluvial lithofacies association. Tetang Formation, near Tetang village (Fig. 3A). Arrows point to examples of imbricated clasts. (C) Imbricated cobble conglomerate of facies B1 and sandy bar flank deposits of facies B2 of braided fluvial lithofacies association. Thakkhola Formation, near Chele village (Fig. 4A). Note the presence of granite clasts (arrows), a common clast-type in axial river deposits of the Thakkhola Formation. (D) Paleosol of facies B3 of braided fluvial lithofacies association with nodular pedogenic carbonate horizon. Thakkhola Formation, near Chele village (Fig. 4A). Black line indicates thickness of massive oxidized mudstone in upper part of paleosol. Arrows point to two nodular carbonate horizons.

gray and grades up into massive gray to red/yellow/gray mudstone, forming a 0.1–1.5-m-thick deposit. These deposits are often stacked to form bodies up to 5 m thick. These deposits usually contain one or more of the following: root traces, bioturbation, plant fossils, hematized zones, and nodular carbonate horizons (Fig. 5D).

#### **Interpretation**

On the basis of bedding thickness, shape, lateral continuity, and stacking patterns, the imbricated and horizontally bedded conglomerate deposits of lithofacies B1 are interpreted as longitudinal bar deposits that filled relatively shallow gravelly channels (e.g., Hein and Walker, 1977). Normal grading of individual beds may have developed during waning flow.

Interbedded sandstones/mudstones of lithofacies B2 may have been deposited on the tops or flanks of bars during waning flow or in

slack-water ponds, such as abandoned channels (Rust, 1972; Miall, 1977).

Lithofacies B3 contains features that are consistent with overbank deposition and subsequent soil development (Miall, 1985). Stacked sequences of alternating overbank deposits and paleosols suggest that river banks were sometimes stable over long periods of time.

#### **Lacustrine Lithofacies Association**

##### **Description**

The lacustrine lithofacies association comprises mudstone (C1) with interbedded sandstone and conglomerate (C2) and carbonate (C3 and C4). These deposits are most abundant in the axial and southeastern parts of the basin. Lithofacies C1 is poorly consolidated, laminated to massive calcareous mudstone (Fig. 5E). Some massive calcareous mudstone beds exhibit exfoliation weathering around

nodular masses (5–12 cm diameter), bioturbation, and plant fossils.

Lithofacies C2 occurs within the mudstone facies as 0.1–0.5-m-thick beds of normally graded or structureless sandstone and clast-supported, pebble conglomerate. These beds are tabular, have sharp erosional bases, and can be traced laterally for tens to >100 m over the length of the outcrop belt. Asymmetric ripple cross-laminae are sometimes preserved in the upper parts of these sandstone beds.

Lithofacies C3 consists of laminated to massive carbonate up to 1.4 m thick and laterally continuous for tens of meters. These carbonate beds are interbedded within braided fluvial lithofacies. The carbonates are micritic and contain ostracods, charophytes, and shell fragments. Petrographic inspection reveals that carbonates contain 10%–50% blocky or sparry calcite.

Lithofacies C4 is massive to laminated carbonate that forms beds from 0.05 to 0.5 m

thick. These deposits are rich in organic matter and often release a petroliferous odor when broken. In thin section, the carbonate is micritic; sparry or blocky recrystallized calcite constitutes up to 50% of the rock. Carbonate beds of lithofacies C4 are stacked to form deposits up to 100 m thick and laterally continuous for as far as 2 km. These carbonates are laterally contiguous with organic-rich mudstones of lithofacies C1.

### Interpretation

The mudstone and sandstone/conglomerate of lithofacies C1 and C2 form packages from 2 to 80 m thick that continue laterally for kilometers. Lithofacies C1 was deposited by fallout of suspended sediment carried by streams feeding into the lakes. The exfoliation-weathering, bioturbated massive mudstones are interpreted as paleosols that developed on the margin of the lake during regression. Lithofacies C2 is interpreted as the deposits of turbidity flows within the lake (Lowe, 1982; Nemeč and Steel, 1984); ripples formed during waning stages of the flow.

Carbonate beds of lithofacies C3 are interpreted as slack-water pond deposits associated with fluvial deposits, on the basis of their limited lateral extent and contiguity with the braided river lithofacies.

We suggest that lithofacies C4 represents profundal lacustrine deposits. Accumulations of organic material are probably associated with seasonal accumulations of phytoplankton that remained unoxidized as a result of stagnant bottom conditions.

## SEDIMENT DISPERSAL PATTERNS

### Paleocurrent Directions

Paleocurrent indicators across the basin are summarized in Figure 6. Paleocurrent data from imbricated cobble-boulder conglomerates in the Tetang Formation in the Ghidiya Khola section (khola means river in Nepali) indicate dominantly westward paleoflow (Fig. 3B). In the Tetang Village section, imbricated pebble conglomerates indicate east-southeastward paleoflow below 80 m in the section, shifting to the south-southeastward up to 100 m and southwestward above 120 m (Fig. 3A).

Along the western edge of the basin, cobble-boulder conglomerates of the Thakkhola Formation indicate dominantly southeast- and eastward paleoflow (Fig. 4A [lower 150 m] and Fig. 4C). Above 150 m in the Chele section, pebble-cobble conglomerates indicate south- to westward paleoflow. Along the axis of the basin, cobble conglomerates indicate

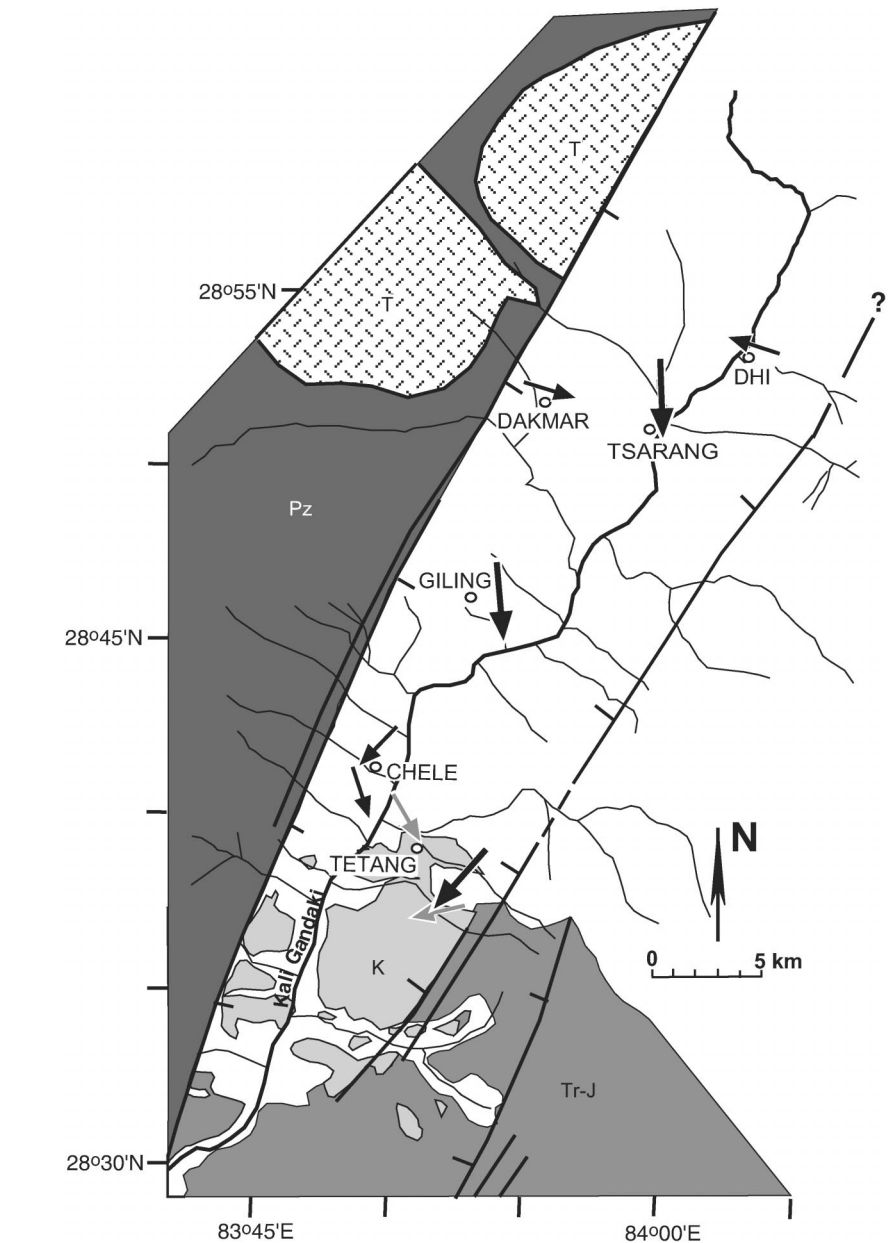


**Figure 6. Paleocurrent map showing average paleoflow direction of axial drainage facies (large arrows) and transverse drainage facies (small arrows) from each measured section in the Tetang Formation (gray arrows) and Thakkhola Formation (black arrows).**

southeast- to southwestward paleoflow (Figs. 4B and 4E). Paleoflow indicated by pebble conglomerates in the northeastern part of the basin was generally toward the west-northwest (Figs. 4D and 6).

### Provenance

Conglomerate provenance indicates a simple unroofing history from Mesozoic and Paleozoic clasts in the Tetang Formation to dominantly Paleozoic, some Mesozoic, and granite

clasts in the Thakkhola Formation. In the Tetang Formation, along the southeastern edge of the basin, clast counts indicate a source region in the Mesozoic rocks exposed in the adjacent footwall that bounds the basin on the east (Fig. 3B). However, in the central part of the basin, conglomerate clasts consist of ~60% Paleozoic phyllites and ~40% Triassic to Jurassic calcareous clastic and carbonate rocks, reflecting rocks exposed in the western footwall (Fig. 3A). Paleocurrent indicators in the Tetang Formation are consistent with the

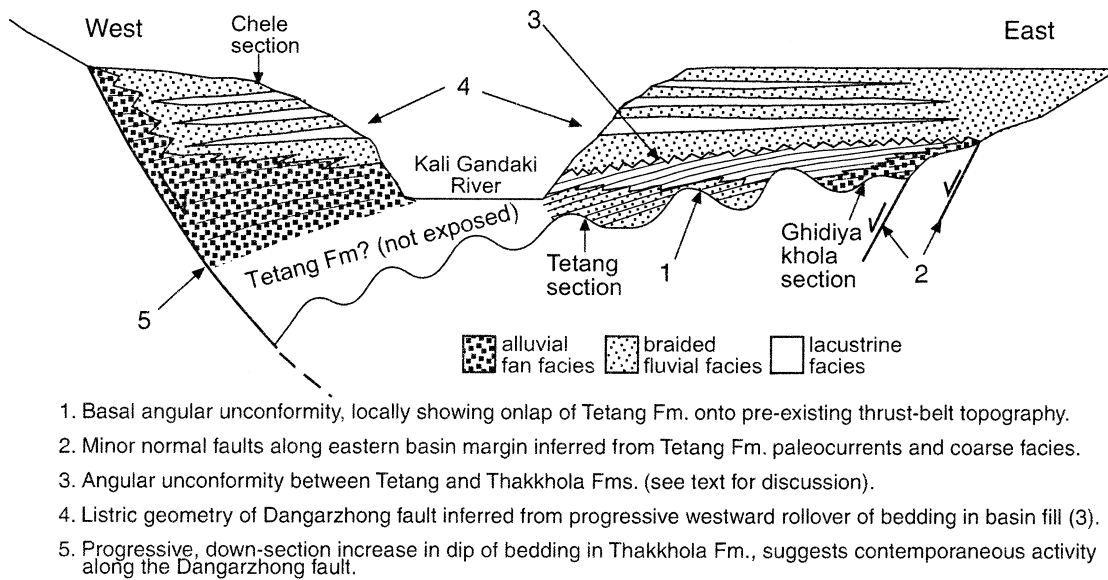


**Figure 7. Schematic cross section through the southern Thakkhola graben, showing important features used to interpret the tectonic history of the basin.**

provenance data (Figs. 3 and 6) and also suggest that clasts deposited in the southeastern part of the basin were derived from the east, whereas clasts deposited in the central part of the basin were derived from the west and north.

In the Thakkhola Formation, along the axis of the basin, cobble conglomerates consist of 60%–75% Paleozoic clasts, 10%–25% Mesozoic clasts, and 10%–25% granite clasts (Fig. 3B [above unconformity] and Fig. 4B). Along the eastern edge of the basin near the town of Dhi, conglomerate clasts are almost entirely Mesozoic (Fig. 4D). Although the basin's eastern margin north of Tetang village has not been mapped, the composition of these conglomerates combined with paleocurrent information suggests that Mesozoic rocks are exposed in the eastern footwall near Dhi (Figs. 4D and 6). Along the fault that bounds the basin on the west, boulder-cobble conglomerates of the Thakkhola Formation contain dominantly Paleozoic and some Mesozoic clasts, consistent with sources in the western footwall. Clasts consist of 60%–98% Paleozoic rocks, and most of the remaining clasts are Mesozoic rocks. In both the Chele and Dakmar sections, a brief incursion of granite clasts is found near the base of the Thakkhola Formation, where granite clasts make up between 10% and 50% of the total clast population (84 m–150 m levels near Chele and 15 m–33 m levels near Dakmar) (Figs. 4A and 4C).

## BASIN EVOLUTION

A model of basin evolution must explain the following features: paleotopography prior to initial sedimentation, growth faults and facies patterns in the Tetang Formation, the angular unconformity between the Tetang and Thakkhola Formations, and growth strata and facies patterns in the Thakkhola Formation. These features are shown in Figure 7 and discussed in the ensuing sections.

### Tetang Formation

The Tetang Formation displays complex stratigraphic patterns associated with remnant paleotopography, with no significant thickening toward the eastern or western basin-bounding faults (Fig. 7). Along the eastern flank of the basin, where the contact relationships are especially well exposed along the Narsing and Ghidiya Kholas, the Tetang Formation tapers and onlaps the Mesozoic basement (Figs. 8 and 9). Thus, the evidence linking deposition of the Tetang Formation with major east-west extension along the present basin-bounding faults is not clear-cut. The apparent restriction of alluvial-fan deposits to the eastern part of the Tetang outcrop area suggests local high-relief topography along the eastern margin of the basin. However, these deposits could also be associated with local, remnant topography that resulted from shortening in the Tethyan fold-thrust belt. Examples in which the Tetang Formation over-

laps remnant topography are superbly exposed along Narsing Khola southeast of Tetang village, where the upper carbonate-rich part of the Tetang Formation thickens abruptly westward off of the crest of a large fold in Mesozoic rocks (Fig. 8). Similarly, a large (~2 km<sup>2</sup>) paleotopographic high directly south of Tetang village separated the two southern outcrop areas from the three northern areas (Fig. 10).

The Tetang Formation records several paleoenvironments, including alluvial fans, small braided rivers and associated floodplains, and large lakes. Early Tetang deposition was dominated by fluvial environments along the axis of the basin and alluvial-fan environments along the eastern margin of the basin. Fluvial conglomerates are pebbly and consist of beds between 0.2 and 0.8 m thick, which are interpreted as bar deposits. Bed thickness indicates that channels were as deep as 0.8 m. Both grain size and channel depth suggest that this river system was much smaller than the modern Kali Gandaki river.

The late Tetang deposition was in an extensive lake system (= 10 km<sup>2</sup>) dominated by carbonate deposition (facies C4) (Figs. 3 and 9). Extremely positive  $\delta^{13}\text{C}$  values ( $\delta^{13}\text{C}_{\text{VPDB}}$  up to 12‰ [VPDB = Vienna Peedee belemnite isotope standard]) in diagenetically altered carbonates of the Tetang Formation (Garziane, 2000) may have resulted from methanogenic processes (e.g., Talbot and Kelts, 1990), which suggests that these lakes had productive surface waters that led to the de-



**Figure 8.** Stratigraphic relationships near Narsing Khola (see Fig. 10 for location). (A) Tetang Formation (Tt) overlies Cretaceous Chuck Formation (K), whereas Cretaceous rocks and Tetang Formation were beveled before deposition of the Thakkhola Formation (Th). (B) Tetang Formation overlying folded Cretaceous rocks.

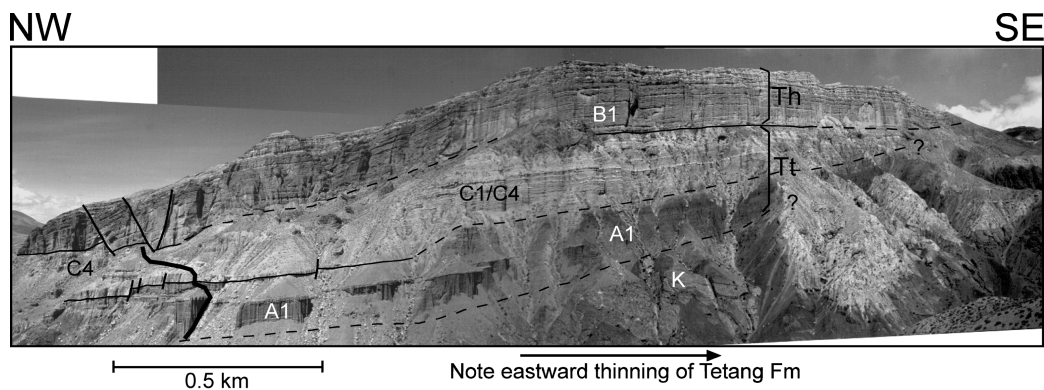


**Figure 9.** Stratigraphic relationships along Ghidiya Khola. Cretaceous Chuck Formation (K), Tetang Formation (Tt), and Thakkhola Formation (Th) (see Fig. 10 for location). Letters indicate lithofacies discussed in text: A1, B1, C1, C4. Thin, solid, subhorizontal lines show lithofacies and formation boundaries, and dashed lines are inferred boundaries. Thick, subvertical lines are minor normal faults, and very thick line shows approximate location of measured section. Note the eastward thinning of Tetang Formation and the lateral extent of axial drainage facies of the Thakkhola Formation.

development of dysaerobic bottom conditions. Tetang lacustrine deposits display shoaling-upward cycles on the order of  $<5$  m and become more widespread through time. The predominance of carbonate deposition, fluctuating lake levels, and increasing lake size suggest balanced-filled to underfilled lake conditions, with limited throughgoing river systems (e.g., Carroll and Bohacs, 1999).

Paleocurrent, provenance, and lithofacies data suggest that Tetang conglomerates were derived from both margins of the basin and deposited in small southward-flowing rivers and small, coarse-grained alluvial fans. Provenance data from the central part of the basin indicate both Paleozoic and Mesozoic source terranes to the north and west. These rocks were almost certainly exposed throughout the

fold-thrust belt prior to deposition of the Tetang Formation, and inherited drainage patterns could have transported clasts from distal regions into the basin.

The strongest evidence for syndepositional normal faulting during Tetang deposition comes from detailed mapping in Narsing and Ghidiya Kholas. Tetang strata have fairly uniform dips of  $18^{\circ}$ – $24^{\circ}$  toward the north-northwest (Fig. 10). Variations of dip are localized around minor normal growth faults (Fig. 11A). These growth faults record several meters to 10 m of offset and are roughly parallel ( $\pm 30^{\circ}$ ) to the eastern and western basin-bounding faults. Larger-offset, northwest-striking normal faults cut both the Tetang and Thakkhola Formations and do not appear to be associated with syntectonic thickness

changes in either unit, suggesting that they postdate deposition (Fig. 10).

Given the absence of evidence for major syndepositional normal faulting during deposition of the Tetang Formation, we suggest that much of the accommodation space for Tetang deposition may have developed as a response to normal faulting and footwall uplift associated with the South Tibetan detachment system (Fig. 12A). Vannay and Hodges (1996) and Godin (1999) reported muscovite  $^{40}\text{Ar}/^{39}\text{Ar}$  ages from the footwall of the Annapurna detachment (part of the South Tibetan detachment system in the Kali Gandaki drainage) that indicate cooling through the muscovite closure temperature between ca. 15 and 13 Ma. Younger muscovite  $^{40}\text{Ar}/^{39}\text{Ar}$  ages between  $12.7 \pm 0.4$  Ma and  $11.8 \pm 0.4$  Ma from

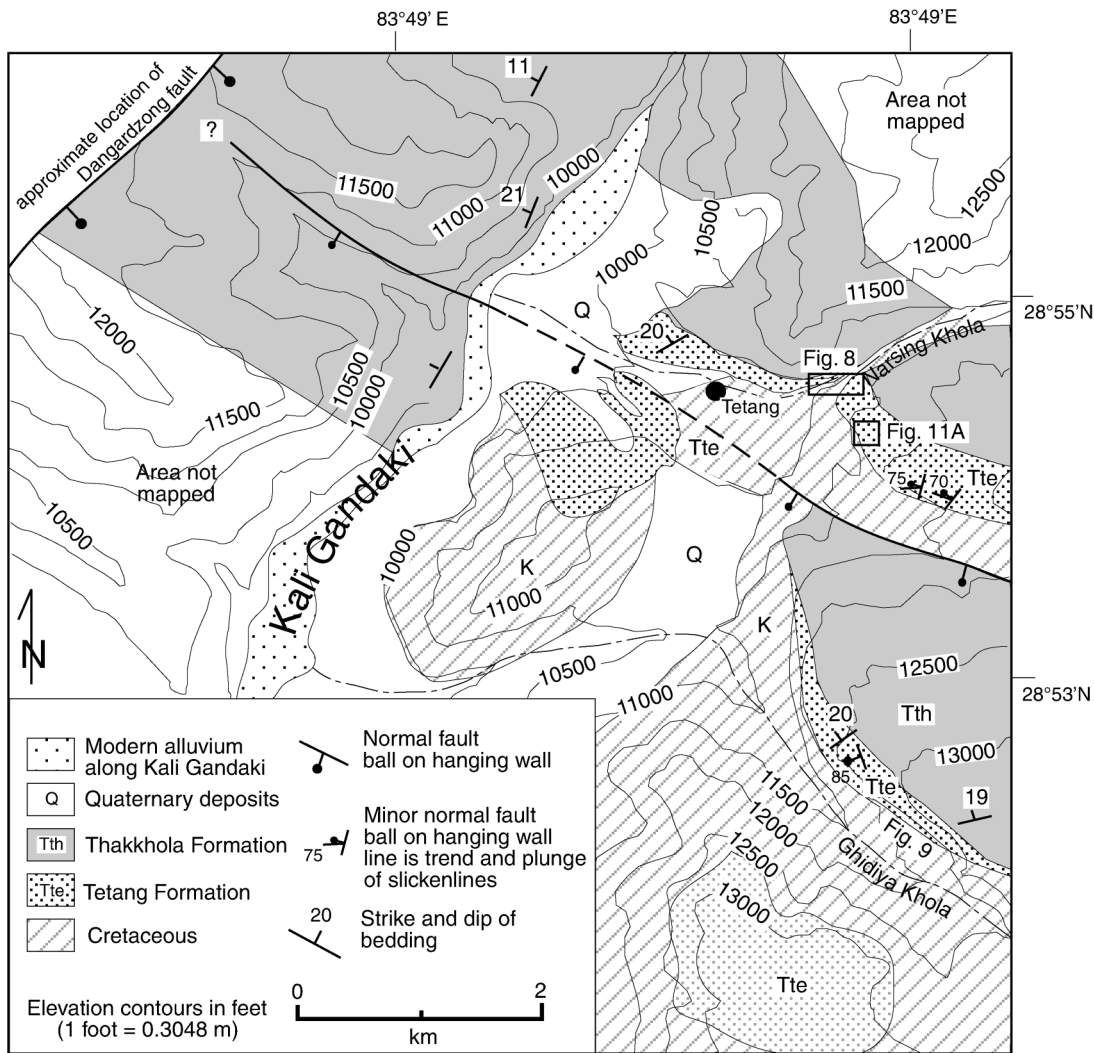


Figure 10. Geologic map of southern part of the Thakkhola graben showing the distribution of the Tetang Formation with respect to Miocene paleotopography developed in the Mesozoic Tethyan Series rocks. Locations of Figures 8, 9, and 11A are shown.

the immediate hanging wall of the detachment have been interpreted as reflecting a hydrothermal event associated with late brittle extension on the Annapurna detachment (Godin, 1999). These ages coincide with initial deposition of the Tetang Formation and suggest that footwall uplift could have produced a structural dam that was capable of ponding drainage to the north and creating large lakes on top of the fold-thrust belt (Fig. 12A). This mechanism could account for the locally thick accumulations of the Tetang Formation and the absence of significant thickening toward either of the basin-bounding faults. Growth faults in the upper Tetang Formation (Fig. 11A) herald the onset of east-west extension, which was subsequently recorded by deposition of the overlying Thakkhola Formation.

#### Development of the Tetang-Thakkhola Angular Unconformity

The Thakkhola Formation overlies the Tetang Formation in angular unconformity (Fig. 7). Tetang strata dip  $\sim 18^\circ$  to  $24^\circ$  to the north-northwest. These strata were rotated into the western basin-bounding fault and beveled prior to deposition of the Thakkhola Formation, which dips  $\sim 15^\circ$  to the northwest at the base of the section, above the unconformity. Fort et al. (1981, 1982) recognized the angular unconformity between the Tetang and Thakkhola Formations near the village of Tetang. This study documents the same unconformity along Ghidiya Khola, which was previously mapped entirely as Tetang Formation (Fort et al., 1981). The contact and facies in the cliffs above Ghidiya Khola (Figs. 9 and 11B) cor-

relate better with imbricated cobble conglomerates at the base of the Thakkhola Formation. Recognition of this unconformity is significant because overlying Thakkhola strata represent the first southward-flowing axial river system, consistent in size with the Kali Gandaki river and containing the first granite clasts (Fig. 3B, top of stratigraphic column). This angular unconformity also represents a temporal gap of  $\geq 2.6$  m.y., beginning at ca. 9.6 Ma and ending after 7 Ma (Garzione et al., 2000a), which may have resulted from incision of the Tetang Formation and Tethyan Series by this large southward-flowing river system. The Tetang Formation was rotated  $\sim 5^\circ$  to the northwest prior to deposition of the Thakkhola Formation, suggesting that significant displacement occurred on the Dangardzong fault during this hiatus.

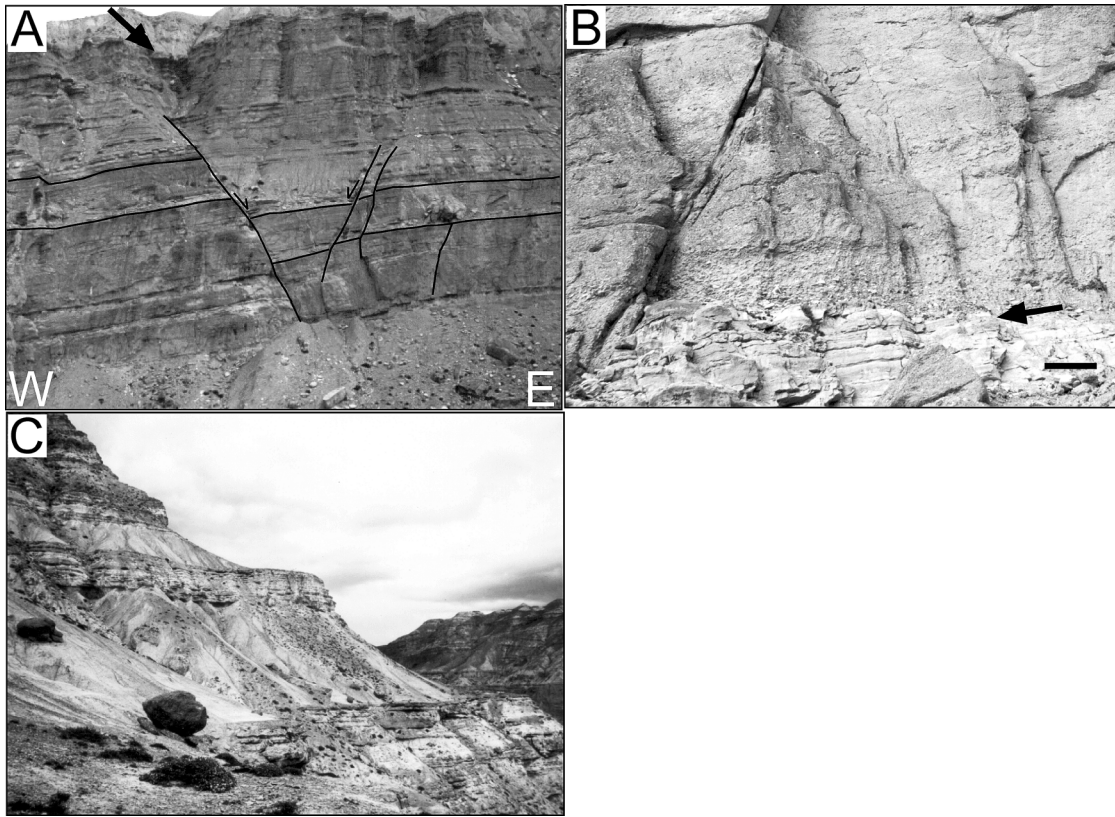


Figure 11. (A) Normal growth faulting in the Tetang Formation (see Fig. 10 for location). Subhorizontal lines show single horizons, broken by normal faults. Note that Tetang deposits are thickened on the downthrown side of the faults. (B) Angular unconformity (arrow) between the Tetang Formation carbonate (lithofacies C4) and Thakkhola Formation cobble conglomerates (lithofacies B1). Black bar represents 1 m. (C) Widespread lacustrine deposits of the Thakkhola Formation. Shown here are two lacustrine intervals that correspond with 285–370 m and 400–430 m in the Chele stratigraphic section (Fig. 4A).

### Thakkhola Formation

The base of the Thakkhola Formation can only be observed above the Tetang Formation and where there are paleotopographic highs in underlying Cretaceous rocks. Along the axis of the basin, the Thakkhola Formation consists of braided fluvial deposits. We gathered clast composition and paleocurrent data from this paleo-river system in three locations: (1) overlying the Tetang Formation along Ghidiya Khola, (2) near the town of Giling, and (3) along Tsarang Khola (Figs. 3B, 4B, and 4E). Cobble conglomerate beds from these deposits, interpreted as longitudinal bars, are 0.2–2 m thick and continue laterally for tens of meters. The thickness of bar deposits indicates that channels were as deep as 2 m. These beds are amalgamated to form lenticular bodies perpendicular to flow that can be traced laterally for hundreds of meters to several kilometers. Grain size, lateral extent, and channel depth suggest that this paleo-river system was comparable in size to the modern Kali Gandaki river. The generally southward paleoflow

recorded in these deposits is the same as the modern Kali Gandaki river. The axial river deposits can be distinguished from small transverse river deposits in the basin by their lateral extent, bedding thickness, and the presence of granite clasts in the axial river conglomerates, probably derived from the Mustang-Mugu granite bodies. We interpret these deposits as evidence for the existence of the paleo-Kali Gandaki river by late Miocene time (ca. 7 Ma) (Fig. 12B). The thickness of the Thakkhola Formation increases markedly from east to west, and bedding generally dips toward the west. In the western part of the basin, adjacent to the Dangardzong fault, the dip of the Thakkhola Formation decreases up-section from as much as  $20^\circ$  at the base of the section to  $<3^\circ$  at the top as a result of growth folding of strata during displacement on the Dangardzong fault (Fig. 7).

Along the western edge of the basin, the Thakkhola Formation consists of alluvial-fan conglomerates, up to 400 m thick, deposited by braided streams, debris flows, and sheet floods (Figs. 4A and 4C), also providing evi-

dence that the Dangardzong fault was active during deposition of the Thakkhola Formation (Fig. 12B). In the northeastern part of the basin, conglomerates with west-northwestward paleoflow directions are interpreted as transverse braided fluvial drainages that flowed toward the axis of the basin (Fig. 4D). Interbedded lacustrine deposits of mudstone and carbonate probably represent paludal deposits associated with these transverse drainages. Conglomerate clasts in these small tributary drainages were derived entirely from Mesozoic rocks, presumably in the eastern footwall.

Three widespread lacustrine units occur throughout the southern part of the basin. In the Chele section, lacustrine intervals occur between 285–370 m, 400–430 m, and 640–685 m (Figs. 4A and 11C) and can be traced laterally for up to 5 km. Axial drainage facies occur below and above these lacustrine deposits. Episodes of lacustrine deposition alternating with axial fluvial deposition indicate periodic damming of this southward-flowing river system (Fig. 12C).

Braided fluvial systems in the upper two

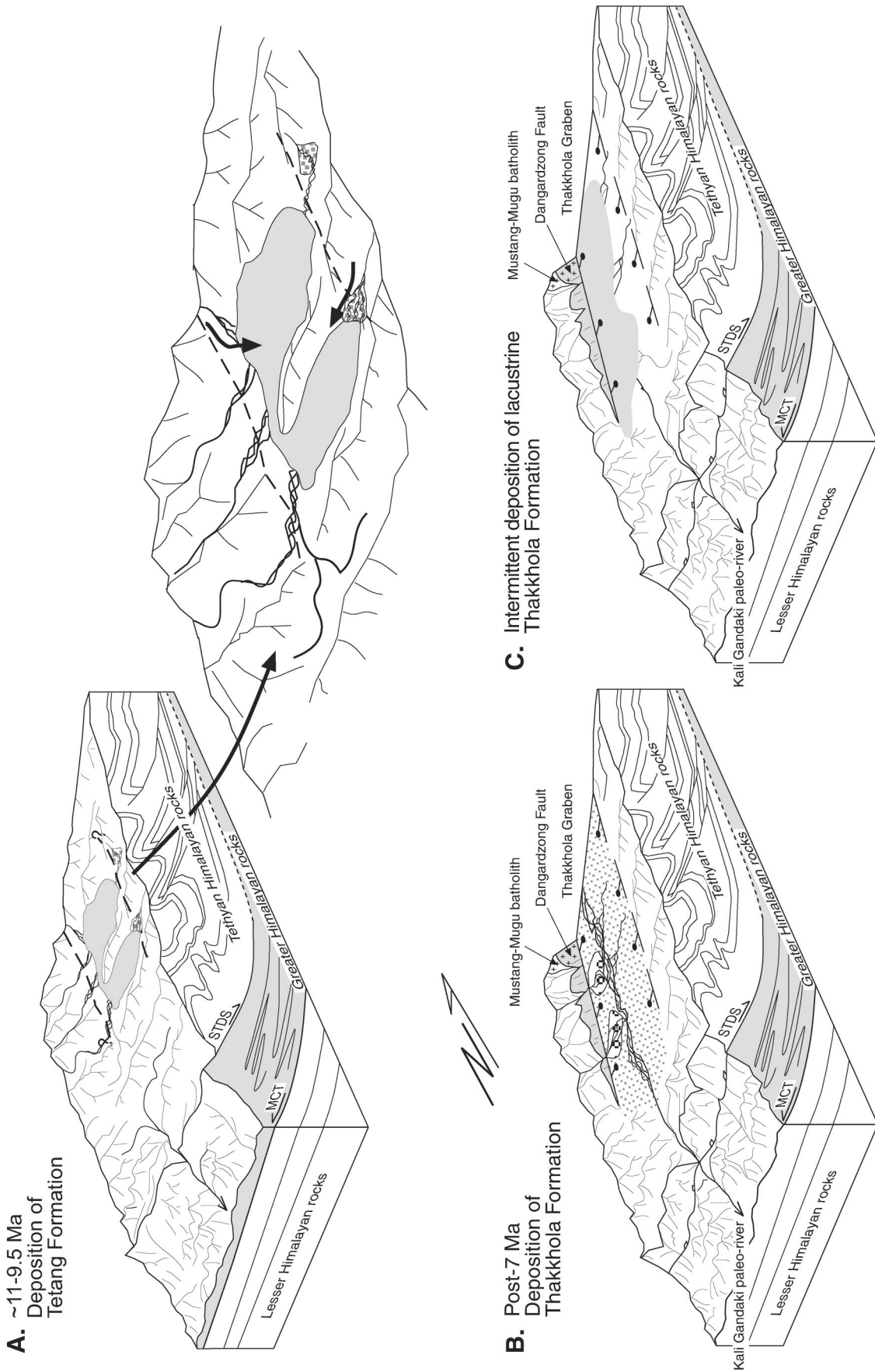


Figure 12. Paleogeographic reconstructions of late Miocene to Pliocene depositional systems and sediment dispersal patterns based on facies distributions, paleocurrent data, and conglomerate clast provenance data shown in Figures 3 and 4. Normal faults are shown as lines with balls on the hanging wall. Dashed lines represent normal faults that may have experienced a minor amount of displacement. See text for discussion.

thirds of the section measured near Chele (Fig. 4A) exhibit generally southwestward paleo-flow directions. These facies lack granite clasts and were deposited by rivers much smaller than the modern Kali Gandaki river. The predominance of Paleozoic clasts in these deposits indicates that the rivers were deriving material from the western margin of the basin. We interpret these deposits as tributary drainages that flowed parallel to the basin axis before joining the paleo-Kali Gandaki river.

Conglomerate provenance in the Thakkhola Formation provides some constraints on exhumation rates in the western footwall. The first granite clasts appear at the base of the Thakkhola Formation in the axial drainage facies. These granites were most likely derived from the Mugu-Mustang plutons along the northwestern margin of the basin (Fig. 2). Le Fort and France-Lanord (1995) determined that the Mugu granite was emplaced at pressures between 2.6 and 4.1 kbar, which indicates depths between ~8 and 12 km. Harrison et al. (1997) obtained a Th-Pb monazite age of  $17.6 \pm 0.3$  Ma for the Mugu pluton. If a conservative age estimate of ca. 5 Ma is assumed for the base of the Thakkhola Formation, exhumation rates of the Mugu pluton were fairly rapid, averaging between ~0.6 and 1 mm/yr between the pluton crystallization age and the depositional age of the Thakkhola Formation.

## DISCUSSION

### Climate Trends

The sedimentary fill of the Thakkhola graben records paleoclimate trends in the southern Tibetan plateau. Several lines of evidence suggest that conditions have become increasingly arid in the Thakkhola graben since deposition began at ca. 11 Ma. Pollen data from the Tetang Formation indicate the presence of abundant pine (*Pinus*), alder (*Alnus*), fir (*Abies*), oak (*Quercus*), hemlock (*Tsuga*), and birch (*Betula*) (Yoshida et al., 1984). Although some pollen may have been transported into the basin by wind, *Tsuga* pollen, which does not persist in the basin today, is less prone to wind transport. Today the graben floor is covered by steppe vegetation, with restricted high-elevation pockets of juniper, pine, and fir (Fort, 1987). Currently, no natural stands of deciduous trees exist in the basin, and the conifers that do persist are restricted to higher elevations, which receive more precipitation.

Paleosol characteristics suggest that conditions were more humid during Tetang deposition than during Thakkhola deposition. The

presence of pedogenic carbonate is generally associated with semiarid or arid climates (e.g., Slate et al., 1996). Lack of pedogenic carbonate in Tetang Formation paleosols associated with fluvial and alluvial-fan lithofacies, in contrast to the abundance of paleosol carbonate nodules in the Thakkhola Formation, suggests that climate may have been more humid during Tetang deposition. In addition, histic horizons and gleyed horizons are more common in the Tetang Formation, suggesting waterlogged conditions.

Oxygen isotopes from carbonates in the Thakkhola graben suggest that during Miocene time this region was as elevated as it is today (~3800–5900 ± 500 m, Garzzone et al., 2000a, 2000b). Environmental changes and depositional changes observed at ca. 8–7 Ma in the Indo-Gangetic foreland, Bengal fan, and Arabian Sea have been attributed to intensification of the Asian monsoon at that time (Quade et al., 1989; Kroon et al., 1991; Prell et al., 1992; Burbank et al., 1993; Derry and France-Lanord, 1996). More recently, stable isotopes of mollusks in Siwalik foreland basin deposits have been interpreted to indicate an intense Asian monsoon prior to 8 Ma, with overall greater annual precipitation, much like modern Burma (Dettman et al., 2001). In monsoon climates, summer monsoon precipitation usually has more negative  $\delta^{18}\text{O}$  values than winter precipitation because the intensity of the rainfall causes a rapid depletion of  $^{18}\text{O}$  in the cloud mass (Rozanski et al., 1993). Very large seasonal variations in  $\delta^{18}\text{O}$  values of mollusks between winter and summer rainfall reflect variations that are greater than modern foreland precipitation (Dettman et al., 2001). Prior to 7 Ma, the  $\delta^{18}\text{O}$  value of winter rainfall was similar to modern rainfall, whereas summer rainfall was more negative than modern by up to several per mil. This finding suggests that the intensity of the summer monsoon was even greater than today. In addition, the middle member of the Siwalik Group (beginning at ca. 11 Ma in western Nepal) displays an increase in channel size and change in channel morphology that suggest an approximately five-fold increase in discharge (DeCelles et al., 1998). This increase in discharge recorded in the middle member of the Siwalik Group is consistent with observations of a more humid climate during deposition of the Tetang Formation. Greater humidity in the Himalaya and Tibet during the late Miocene may explain the presence of large mammalian fauna and more humid-climate flora in other basins on the Tibetan plateau (e.g., Chen, 1981; Xu, 1981; Li et al., 1995).

Perhaps the most important implication of

an elevated and more humid Tibetan plateau prior to 8 Ma is that our current ideas about the timing of uplift of the plateau and related climate change are too simple. It is generally accepted that intensification of the Asian monsoon coincided with uplift of the plateau at ca. 8 Ma (e.g., Prell and Kutzbach, 1992; Raymo and Ruddiman, 1992; Harrison et al., 1992; Molnar et al., 1993). However, paleoclimate and paleoelevation prior to 8 Ma are still poorly understood. Future studies will likely reveal that the Tibetan plateau had a more complicated uplift history than we currently understand and that the intensification of the Asian monsoon occurred earlier than 8 Ma.

### Southward Drainage of the Kali Gandaki River

Facies distributions and paleocurrent directions in the Thakkhola graben, at the base of the Thakkhola Formation, document the onset of southward axial drainage, which was similar to the size of the modern Kali Gandaki river. Paleocurrent indicators from the lower Tetang Formation in the central part of the basin also indicate southward-flowing rivers, but facies distributions in the upper Tetang Formation suggest that drainage became increasingly restricted.

Several intervals of widespread lacustrine deposition within the Thakkhola Formation (Fig. 11C) indicate intermittent damming of the axial drainage system or rapid subsidence along the Dangardzong fault. A few mechanisms could explain the lack of a large southward axial drainage system during Tetang and Thakkhola deposition: (1) glacial damming, (2) northward paleoslope and paleodrainage, and (3) structural damming. Glacial damming or a northward paleoslope are possible, but unlikely, mechanisms for the lack of a southward axial drainage system during deposition of the Tetang Formation. Glacial advance and retreat have been suggested as a mechanism for Quaternary sediment damming and incision along the Kali Gandaki river (e.g., Fort et al., 1982; Iwata, 1984). However, because there is no evidence for glacial deposition in the Tetang Formation or Thakkhola Formation, we view this as an unlikely mechanism for sediment damming during that time. A northward paleoslope also seems unlikely in view of the absence of northward paleoflow indicators and clasts derived from the Greater Himalayan rocks. On the contrary, southward paleoflow of braided rivers in both formations and the development of lakes in the southern part of the graben indicate a southward paleoslope.

Abundant structural and thermochronological evidence suggests growth of structures south of Thakkhola graben that could have caused structural damming. Initial displacement on the Main Central thrust in central Nepal occurred by ca. 22.5 Ma at about the same time as initial extension on the South Tibetan detachment system (Hodges et al., 1996; Coleman, 1998). Younger muscovite  $^{40}\text{Ar}/^{39}\text{Ar}$  ages between  $12.7 \pm 0.4$  Ma and  $11.8 \pm 0.4$  Ma from the immediate hanging wall of the detachment (Godin, 1999) and the identification of Quaternary normal faulting along the detachment (Hurtado et al., 2001) are evidence of recent brittle reactivation of the detachment system, which could have been responsible for the closed-basin conditions during Tetang deposition. Either (1) headward erosion through the Greater Himalaya south of the detachment system or, (2) the rupture of the detachment system and Greater Himalaya by the Dangardzong fault could have breached this structural dam. The mapping of Colchen et al. (1986) shows the southern termination of east-west extensional faults associated with the Thakkhola graben within Greater Himalayan rocks, whereas mapping by Hurtado et al. (2001) terminates Thakkhola graben normal faults at the South Tibetan detachment. Determining the validity of either of these interpretations is crucial to understanding the development of southward drainage of the Kali Gandaki river and the relationship between grabens in the southern Tibetan plateau and the South Tibetan detachment system.

## CONCLUSIONS

1. Basin fill of the Thakkhola graben provides a record of paleoenvironment and the development of east-west extension in the southern Tibetan plateau. The Tetang Formation (ca. 11–9.6 Ma) is up to 230 m thick and consists of pebbly braided fluvial deposits, which grade up into lacustrine deposits. Along the eastern edge of the basin, sheetflood-dominated alluvial fans constitute the lower part of the Tetang Formation. The Tetang and overlying Thakkhola Formations are separated by an angular unconformity represented by an  $\sim 5^\circ$  northwest rotation and beveling of Tetang strata, possibly related to initial activity on the Dangardzong fault and development of a southward, axial, throughgoing drainage system. The younger Thakkhola Formation (younger than 7 Ma) is up to 800 m thick and consists of cobbly, braided fluvial deposits and intermittent widespread lacustrine deposits along the axis of the basin. Fluvial and debris-flow alluvial-fan deposits are restricted to the west-

ern edge of the basin, and pebbly cobbly deposits show that braided rivers fed into the basin off of its eastern edge.

2. North-striking normal growth faulting within the Tetang Formation indicates that minor east-west extension occurred during Tetang deposition, although stratigraphic thickening and rotation associated with the major basin-bounding faults was not observed. The Dangardzong fault that bounds the western edge of the basin was active prior to and throughout deposition of the Thakkhola Formation.

3. Deposition of the Tetang Formation took place in several restricted basins, owing to paleotopography developed in deformed Tethyan Series rocks. During deposition of the lower Tetang Formation, small braided rivers in the central part of the basin flowed mainly southward. Lacustrine deposition became more widespread later, as shown up-section in the Tetang Formation. Late Miocene brittle motion on the Annapurna detachment, south of the Thakkhola graben, may have formed a structural dam, which caused the ponding of drainage to the north and led to the development of large lakes within the Tethyan fold-thrust belt. By the base of the Thakkhola Formation, a large axial river system with southward paleoflow had developed. Southward drainage of the paleo-Kali Gandaki river could have developed by headward erosion of the Greater Himalaya that breached the South Tibetan detachment system or by extensional faults that cut through the detachment system and greater Himalayan rocks. Several episodes of widespread lacustrine deposition indicate that this river system experienced periodic damming perhaps by renewed activity on the Annapurna detachment.

4. A more humid climate during deposition of Tetang Formation is inferred from the greater abundance of conifer and deciduous pollen compared to today, the lack of pedogenic carbonate, and common histic and gleyed paleosol horizons. Environmental change in the Thakkhola graben between deposition of the Tetang and Thakkhola formation correlates with changes in climate observed in the Siwalik foreland basin, Arabian Sea, and Bay of Bengal. Both evidence from the Thakkhola graben that the southern Tibetan plateau was already elevated by ca. 11 Ma (Garzione et al., 2000a, 2000b) and evidence for intense summer rainfall and dry winters by 10.7 Ma in the Himalayan foreland (Dettman et al., 2001) suggest that by this time a strong south Asian monsoon had developed.

## ACKNOWLEDGMENTS

This project was supported by the National Security Education Program, the Geological Society of America Graduate Research Fund, the GeoStructure Partnership at the University of Arizona (including BP, ExxonMobil, and Conoco), and the Institute for the Study of Planet Earth at the University of Arizona. We thank Jay Quade and David Dettman for insightful discussions and for the use of their labs to carry out the stable isotope analyses. We also thank José Hurtado for helpful discussions on the geology of the Thakkhola graben. We thank Paul Heller, Brad Ritts, and an anonymous reviewer for helping us improve the manuscript.

## REFERENCES CITED

- Armijo, R., Tapponnier, P., Mercier, J.L., and Han, T., 1986, Quaternary extension in southern Tibet: Field observation and tectonic implications: *Journal of Geophysical Research*, v. 91, p. 13,803–13,872.
- Blisniuk, P.M., Hacker, B.R., Glodny, J., Ratschbacher, L., Wu, Z., McWilliams, M.O., and Calvert, A., 2001, Normal faulting in central Tibet: *Nature*, v. 412, p. 628–632.
- Burbank, D.W., Derry, L.A., and France-Lanord, C., 1993, Reduced Himalayan sediment production 8 Myr ago despite an intensified monsoon: *Nature*, v. 364, p. 48–50.
- Burchfiel, B.C., Zhiliang, C., Hodges, K.V., Yuping, L., Royden, L.H., Changrong, D., and Jiene, X., 1992, The south Tibetan detachment system, Himalayan orogen: Extension contemporaneous with and parallel to shortening in a collisional mountain belt: *Geological Society of America Special Paper* 269, 51 p.
- Burg, J.P., and Chen, G.M., 1984, Tectonics and structural zonation of southern Tibet: *Nature*, v. 311, p. 219–223.
- Carroll, A.R., and Bohacs, K.M., 1999, Stratigraphic classification of ancient lakes: Balancing tectonic and climatic controls: *Geology*, v. 27, p. 99–102.
- Catlos, E.J., Harrison, T.M., Kohn, M.J., Grove, M., Ryerson, F.J., Manning, C., and Upreti, B.N., 2001, Geochronologic and thermobarometric constraints on the evolution of the Main Central thrust, central Nepal Himalaya: *Journal of Geophysical Research*, v. 106, p. 16,777–16,204.
- Cerling, T.E., Harris, J.M., MacFadden, B.J., Leakey, M.G., Quade, J., Eisenmann, V., and Ehleringer, J.R., 1997, Global vegetation change through the Miocene/Pliocene boundary: *Nature*, v. 389, p. 153–158.
- Chen, W.Y., 1981, Natural environment of the Pliocene basin in Gyirong, Xizang, in Liu, D.S., ed., *Geological and ecological studies of the Qinghai-Xizang plateau*, Volume I: Beijing, Science Press, p. 343–352.
- Colchen, M., 1999, The Thakkhola-Mustang graben in Nepal and the late Cenozoic extension in the Higher Himalayas: *Journal of Asian Earth Sciences*, v. 17, p. 683–702.
- Colchen, M., LeFort, P., and Pêcher, A., 1986, Annapurna-Manaslu-Ganesh Himal: Centre National de la Recherche Scientifique, Paris, 136 p.
- Coleman, M.E., 1998, U-Pb constraints on Oligocene–Miocene deformation and anatexis, Marsyangdi Valley, central Nepalese Himalaya: *American Journal of Science*, v. 298, p. 553–571.
- Coleman, M., and Hodges, K., 1995, Evidence for Tibetan plateau uplift before 14 Myr ago from a new minimum age for east-west extension: *Nature*, v. 374, p. 49–52.
- DeCelles, P.G., Gray, M.B., Ridgeway, K.D., Cole, R.B., Pivnik, D.A., Pequera, N., and Srivastava, P., 1991, Controls on synorogenic alluvial-fan architecture, Beartooth Conglomerate (Paleocene), Wyoming and Montana: *Sedimentology*, v. 38, p. 567–590.
- DeCelles, P.G., Gehrels, G.E., Quade, J., Ojha, T.P., Kapp, P.A., and Upreti, B.N., 1998, Neogene foreland basin deposits, erosional unroofing, and kinematic history of

- the Himalayan fold-thrust belt, western Nepal: Geological Society of America Bulletin, v. 110, p. 2–21.
- DeCelles, P.G., Robinson, D.M., Quade, J., Ojha, T.P., Garzzone, C.N., Copeland, P., and Upreti, B.N., 2001, Stratigraphy, structure, and tectonic evolution of the Himalayan fold-thrust belt in western Nepal: Tectonics, v. 20, p. 487–509.
- Derry, L.A., and France-Lanord, C., 1996, Neogene Himalayan weathering history and river  $^{87}\text{Sr}/^{86}\text{Sr}$ : Impact on the marine Sr record: Earth and Planetary Science Letters, v. 142, p. 59–74.
- Dettman, D.L., Kohn, M.J., Quade, J., Ryerson, F.J., Ojha, T.P., and Hamidullah, S., 2001, Seasonal stable isotope evidence for a strong Asian monsoon throughout the past 10.7 m.y.: Geology, v. 29, p. 31–34.
- Dhital, M.R., and Kizaki, K., 1987, Structural aspect of the northern Dang, Lesser Himalaya: University of the Ryukyus, Bulletin of the College of Science, v. 45, p. 159–182.
- England, P.C., and Houseman, G.A., 1989, Extension during continental convergence, with application to the Tibetan plateau: Journal of Geophysical Research, v. 94, 17,561–17,579.
- Fielding, E.J., Isacks, B.L., Barazangi, M., and Duncan, C., 1994, How flat is Tibet? Geology, v. 22, p. 163–167.
- Fort, M., 1987, Geomorphic and hazards mapping in the dry, continental Himalaya: 1:50,000 maps of Mustang district, Nepal: Mountain research and development, v. 7, p. 222–238.
- Fort, M., Bassoullet, J.P., Colchen, M., and Freydet, P., 1981, Sedimentological and structural evolution of the Thakkhola-Mustang graben (Nepal Himalaya) during late Neogene and Pleistocene: Calcutta, India, Geological Survey of India, Neogene/Quaternary Boundary Field Conference, India, 1979, Proceeding, p. 25–35.
- Fort, M., Freydet, P., and Colchen, M., 1982, Structural and sedimentological evolution of the Thakkhola Mustang graben (Nepal Himalayas): Zeitschrift für Geomorphologie, v. 42, p. 75–98.
- Gansser, A., 1964, Geology of the Himalayas: London, Interscience, 289 p.
- Garzzone, C.N., 2000, Tectonic and paleoelevation history of the Thakkhola graben and implications for the evolution of the southern Tibetan plateau [Ph.D. thesis]: Tucson, University of Arizona, 146 p.
- Garzzone, C.N., Dettman, D.L., Quade, J., DeCelles, P.G., and Butler, R.F., 2000a, High times on the Tibetan plateau: Paleoelevation of the Thakkhola graben, Nepal: Geology, v. 28, p. 339–342.
- Garzzone, C.N., Quade, J., DeCelles, P.G., and English, N.B., 2000b, Predicting paleoelevation of Tibet and the Himalaya from  $\delta^{18}\text{O}$  vs. altitude gradients in meteoric water across the Nepal Himalaya: Earth and Planetary Science Letters, v. 183, p. 215–229.
- Godin, L., 1999, Tectonic evolution of the Tethyan sedimentary sequence in the Annapurna area, central Nepal Himalaya [Ph.D. thesis]: Carleton University, 219 p.
- Godin, L., Brown, R.L., and Hammer, S., 1999, High strain zone in the hanging wall of the Annapurna detachment, central Nepal Himalaya, in Macfarlane, A., Sorkhabi, R.B., and Quade, J., eds., Himalaya and Tibet: Mountain roots to mountain tops: Geological Society of America Special Paper 328, p. 199–210.
- Guillot, S., 1999, An overview of the metamorphic evolution in central Nepal: Journal of Asian Earth Sciences, v. 17, p. 713–725.
- Harrison, T.M., Copeland, P., Kidd, W.F.S., and Yin, A., 1992, Raising Tibet: Science, v. 255, p. 1663–1670.
- Harrison, T.M., Copeland, P., Kidd, W.F.S., and Lovera, O.M., 1995, Activation of the Nyainqentanghla shear zone: Implications for uplift of the southern Tibetan plateau: Tectonics, v. 14, p. 658–676.
- Harrison, T.M., Lovera, O.M., and Grove, M., 1997, New insights into the origin of two contrasting Himalayan granite belts: Geology, v. 25, p. 899–902.
- Hauck, M.L., Nelson, K.D., Brown, L.D., Zhao, W., and Ross, A.R., 1998, Crustal structure of the Himalayan orogen at  $\sim 90^\circ$  east longitude from Project INDEPTH deep reflection profiles: Tectonics, v. 17, p. 481–500.
- Hein, F.J., and Walker, R.G., 1977, Bar evolution and development of stratification in the gravelly braided Kicking Horse River, British Columbia: Canadian Journal of Earth Sciences, v. 14, p. 562–570.
- Hodges, K.V., 2000, Tectonics of the Himalaya and southern Tibet from two perspectives: Geological Society of America Bulletin, v. 112, p. 324–350.
- Hodges, K.V., and Silverburg, D.S., 1988, Thermal evolution of the Greater Himalaya, Garhwal, India: Tectonics, v. 7, p. 583–600.
- Hodges, K.V., Parrish, R.R., and Searle, M.P., 1996, Tectonic evolution of the central Annapurna Range, Nepalese Himalayas: Tectonics, v. 15, p. 1264–1291.
- Hoorn, C., Ojha, T., and Quade, J., 2000, Palynological evidence for vegetation development and climatic change in Sub-Himalayan zone (Neogene, central Nepal): Palaeogeography, Palaeoclimatology, Palaeoecology, v. 163, p. 133–161.
- Horton, B.K., and Schmitt, J.G., 1996, Sedimentology of a lacustrine fan-delta system, Miocene Horse Camp Formation, Nevada, USA: Sedimentology, v. 43, p. 133–155.
- Hubbard, M.S., and Harrison, T.M., 1989,  $^{40}\text{Ar}/^{39}\text{Ar}$  constraints on deformation and metamorphism in the Main Central thrust zone and Tibetan slab, eastern Nepal Himalaya: Tectonics, v. 8, p. 865–880.
- Hurtado, J.M., Hodges, K.V., and Whipple, K.X., 2001, Neotectonics of the Thakkhola graben and implications for recent activity on the South Tibetan fault system in the central Nepal Himalaya: Geological Society of America Bulletin, v. 13, p. 222–240.
- Iwata, S., 1984, Geomorphology of the Thakkhola-Muktinath region, central Nepal, and its late Quaternary history: Geographical Reports of the Tokyo Metropolitan University, v. 19, p. 25–42.
- Johnson, M.R.W., Oliver, G.J.H., Parrish, R.R., and Johnson, S.P., 2001, Synthrusting metamorphism, cooling, and erosion of the Himalayan Kathmandu Complex, Nepal: Tectonics, v. 20, p. 394–415.
- Kroon, D., Steens, T., and Troelstra, S.R., 1991, Onset of monsoonal related uplift in the western Arabian sea as revealed by planktonic foraminifera, in Prell, W.L., Niituma, N. et al., Proceedings of the Ocean Drilling Program, Scientific results, Volume 117: College Station, Texas, Ocean Drilling Program, p. 257–263.
- Le Fort, P., 1986, Metamorphism and magmatism during the Himalayan collision, in Coward, M.P., and Ries, A.C., eds., Collision tectonics: Geological Society [London] Special Publication 19, p. 159–172.
- Le Fort, P., and France-Lanord, C., 1995, Granites from Mustang and surrounding regions (central Nepal): Journal of Nepal Geological Society, v. 11, p. 53–57.
- Li Jijun, editor, 1995, Uplift of Qinghai-Xizang (Tibet) plateau and global change: Lanzhou, China, Lanzhou University Press, 207 p.
- Lowe, D.R., 1982, Sediment gravity flows: II. Depositional models with special reference to the deposits of high-density turbidity currents: Journal of Sedimentary Petrology, v. 52, p. 279–297.
- McCaffrey, R., and Nabelek, J., 1998, Role of oblique convergence in the active deformation of the Himalayas and southern Tibetan plateau: Geology, v. 26, p. 691–694.
- Miall, A.D., 1977, A review of the braided river depositional environment: Earth-Science Reviews, v. 13, p. 1–62.
- Miall, A.D., 1985, Architectural-element analysis: A new method of facies analysis applied to fluvial deposits: Earth-Science Reviews, v. 22, p. 261–308.
- Molnar, P., and Lyon-Caen, H., 1988, Some simple physical aspects of the support, structure, and evolution of mountain belts, in Clark, S., Burchfiel, B.C., and Suppe, J., eds., Processes in Continental Lithospheric Deformation: Geological Society of America Special Paper 218, p. 179–207.
- Molnar, P., and Tapponnier, P., 1978, Active tectonics of Tibet: Journal of Geophysical Research, v. 83, p. 5361–5375.
- Molnar, P., England, P., and Martinod, J., 1993, Mantle dynamics, uplift of the Tibetan plateau, and the Indian monsoon: Reviews of Geophysics, v. 31, p. 357–396.
- Mugnier, J.L., Mascle, G., and Faucher, T., 1993, Structure of the Siwaliks of western Nepal: An intracontinental accretionary prism: International Geology Reviews, v. 35, p. 32–47.
- Murphy, M.A., and Harrison, T.M., 1999, The relationship between leucogranite magmatism and the Qomolungma detachment in the Rongbuk Valley, south Tibet: Geology, v. 27, p. 831–834.
- Nemec, W., and Steel, R.J., 1984, Alluvial and coastal conglomerates: Their significant features and some comments on gravelly mass-flow deposits, in Kloster, E.H., and Steel, R.J., eds., Sedimentology of gravels and conglomerates: Canadian Society of Petroleum Geologists Memoir 10, p. 1–31.
- Ni, J., and York, J., 1978, Late Cenozoic tectonics of the Tibetan plateau: Journal of Geophysical Research, v. 83, p. 5377–5384.
- Pan, Y., and Kidd, W.F.S., 1992, Nyainqentanghla shear zone: A late Miocene extensional detachment in the southern Tibetan plateau: Geology, v. 20, p. 775–778.
- Prell, W.L., and Kutzbach, J.E., 1992, Sensitivity of the Indian monsoon to forcing parameters and implications for its evolution: Nature, v. 360, p. 647–652.
- Prell, W.L., Murray, D.W., Clemens, S.C., and Anderson, D.M., 1992, Evolution and variability of the Indian Ocean summer monsoon: Evidence from the western Arabian Sea drilling program, in Duncan, R.A. et al., eds., Synthesis of results from scientific drilling in the Indian Ocean: American Geophysical Union Geophysical Monograph 70, 447–469.
- Quade, J., Cerling, T.E., and Bowman, J.R., 1989, Development of Asian monsoon revealed by marked ecological shift during the latest Miocene in northern Pakistan: Nature, v. 342, p. 163–166.
- Quade, J., Cater, J.M.L., Ojha, T.P., Adam, J., and Harrison, T.M., 1995, Late Miocene environmental change in Nepal and the northern Indian subcontinent: Stable isotopic evidence from paleosols: Geological Society of America Bulletin, v. 107, p. 1381–1397.
- Ratschbacher, L., Frisch, W., Liu Guanghua, and Chen Chengsheng, 1994, Distributed deformation in southern and western Tibet during and after the India-Asia collision: Journal of Geophysical Research, v. 99, p. 19,917–19,945.
- Raymo, M.E., and Ruddiman, W.F., 1992, Tectonic forcing of late Cenozoic climate: Nature, v. 359, p. 117–122.
- Royden, L.H., Burchfiel, C., King, R.W., Wang, E., Chen, Z., Shen, F., and Liu, Y., 1997, Surface deformation and lower crustal flow in eastern Tibet: Science, v. 276, p. 788–790.
- Rozanski, K., Araguás-Araguás, L., and Gonfiantini, R., 1993, Isotopic patterns in modern global precipitation, in Swart, P., McKenzie, J.A., and Lohman, K.C., eds., Continental indicators of climate, Proceedings of Chapman Conference, Jackson Hole, Wyoming: American Geophysical Union Geophysical Monograph 78, p. 1–36.
- Rust, B.R., 1972, Structure and process in a braided river: Sedimentology, v. 18, p. 221–245.
- Schelling, D., 1992, The tectonostratigraphy and structure of the eastern Nepal Himalaya: Tectonics, v. 11, p. 925–943.
- Searle, M.P., 1986, Structural evolution and sequence of thrusting in the High Himalaya, Tibetan Tethys, and Indus suture zones of Zaskar and Ladakh, western Himalaya: Journal of Structural Geology, v. 8, p. 923–936.
- Seeber, L., and Pécher, A., 1998, Strain partitioning along the Himalayan arc and the Nanga Parbat antiform: Geology, v. 26, p. 791–794.
- Slate, J.L., Smith, G.A., Wang, Y., and Cerling, T.E., 1996, Carbonate-paleosol genesis in the Plió-Pleistocene St. David Formation, southeastern Arizona: Journal of Sedimentary Research, v. 66, p. 85–94.
- Sohn, Y.K., 1997, On traction-carpet sedimentation: Journal of Sedimentary Research, v. 67, p. 502–509.
- Srivastava, P., and Mitra, G., 1994, Thrust geometries and deep structure of the outer and lesser Himalaya, Kumaon and Garhwal (India): Implications for evolution of the Himalayan fold thrust belt: Tectonics, v. 13, p. 89–109.
- Stöcklin, J., 1980, Geology of Nepal and its regional frame: Geological Society of London Journal, v. 137, p. 1–34.

- Talbot, M.R., and Kelts, K., 1990, Paleolimnological signatures from carbon and oxygen isotopic ratios in carbonates from organic carbon-rich lacustrine sediments, *in* Katz, B.J., ed., Lacustrine basin exploration—Case studies and modern analogs: American Association of Petroleum Geologists Memoir 50, p. 99–112.
- Todd, S.P., 1989, Stream-driven, high-density gravelly traction carpets: Possible deposits in the Trabeg Conglomerate Formation, southwest Ireland and some theoretical considerations of their origin: *Sedimentology*, v. 36, p. 513–530.
- Valdiya, K.S., 1980, Geology of the Kumaon Lesser Himalaya: Wadia Institute of Himalayan Geology, 291 p.
- Vannay, J.C., and Hodges, K.V., 1996, Tectonometamorphic evolution of the Himalayan metamorphic core between Annapurna and Dhaulagiri, central Nepal, *Journal of Metamorphic Geology*, v. 14, p. 635–656.
- Williams, H., Turner, S., Kelley, S., and Harris, N., 2001, Age and composition of dikes in southern Tibet: New constraints on the timing of east-west extension and its relationship to postcollisional volcanism, v. 29, p. 339–342.
- Xu Ren, 1981, Vegetational changes in the past and the uplift of the Qinghai-Xizang Plateau, *in* Geological and geological studies of the Qinghai-Xizang plateau, Volume I, Geology, geological history, and origin of Qinghai-Xizang Plateau: Beijing, Science Press, p. 139–144.
- Yin, A., 2000, Mode of Cenozoic east-west extension in Tibet suggesting a common origin of rifts in Asia during the Indo-Asian collision, v. 105, p. 21,745–21,759.
- Yin, A., Kapp, P.A., Murphy, M.A., Manning, C.E., Harrison, T.M., Grove, M., Ding Lin, Deng Xi-Guang, Wu Cun-Ming, 1999, Significant late Neogene east-west extension in northern Tibet: *Geology*, v. 27, p. 787–790.
- Yoshida, M., Igarashi, Y., Arita, K., Hayashi, D., and Sharma, T., 1984, Magnetostratigraphic and pollen analytic studies of the Takmar series, Nepal Himalayas: *Nepal Geological Society Journal*, v. 4, p. 101–120.

MANUSCRIPT RECEIVED BY THE SOCIETY 13 APRIL 2001

REVISED MANUSCRIPT RECEIVED 29 APRIL 2002

MANUSCRIPT ACCEPTED 28 JUNE 2002

Printed in the USA